HHS Public Access

Author manuscript

Health Phys. Author manuscript; available in PMC 2016 November 01.

Published in final edited form as:

Health Phys. 2015 November ; 109(5): 452–465. doi:10.1097/HP.0000000000000346.

Citrulline as a biomarker in the murine total-body irradiation model: correlation of circulating and tissue citrulline to small intestine epithelial histopathology

Jace W. Jones[*], **Gregory Tudor**[†], **Fei Li**[*], **Yan Tong**[‡], **Barry Katz**[‡], **Ann M. Farese**[§], **Thomas J. MacVittie**[§], **Catherine Booth**[†], and **Maureen A. Kane**[*]

[*]University of Maryland, School of Pharmacy, Department of Pharmaceutical Sciences, Baltimore, MD

[†]Epistem Ltd, Manchester, UK

[‡]Indiana University, School of Medicine and Richard M. Fairbanks School of Public Health, Department of Biostatistics, Indianapolis, IN

[§]University of Maryland, School of Medicine, Department of Radiation Oncology, Baltimore, MD

Abstract

The use of plasma citrulline as a biomarker for gastrointestinal acute radiation syndrome via exposure to total-body irradiation in a murine model was investigated. The radiation exposure covered lethal, mid-lethal, and sub-lethal gastrointestinal acute radiation syndrome. Plasma citrulline profiles were generated over the first 6 days following total-body irradiation exposure of 6–15 Gy. In addition, plasma citrulline was comprehensively evaluated in the context of matching small intestine citrulline and histopathology. Higher plasma citrulline was significantly associated with lower irradiation doses over the first 6 days following the irradiation insult. Furthermore, higher plasma citrulline was significantly associated with higher crypt survival. The correlation of the plasma citrulline to crypt survival was more robust for higher irradiation doses and for later time points. The data suggested plasma citrulline was most informative for reflecting gastrointestinal injury resulting from exposure to 9–15 Gy total-body irradiation covering time-points 2 to 5 days post the irradiation insult.

Keywords

biological indicators; radiation damage; gastrointestinal tract; whole body irradiation

INTRODUCTION

The search, identification, and validation of organ-specific biomarkers is a challenging endeavor yet one that has potentially significant impact in prognosis and/or diagnosis of organ-specific diseases or injuries. One such organ-specific injury in need of organ-specific

Correspondence: Maureen A. Kane, University of Maryland, School of Pharmacy, Department of Pharmaceutical Sciences, 20 N. Pine Street, Room 723, Baltimore, MD 21201, Phone: (410) 706-5097, Fax: (410) 706-0886, mkane@rx.umaryland.edu.

biomarker(s) is the acute effect of high-dose irradiation (IR) on the gastrointestinal (GI) tract, commonly referred to as GI acute radiation syndrome (ARS). Exposure to radiation has received considerable attention recently in light of real and/or potential accidents (e.g., equipment malfunction at a nuclear power plant) or deliberate actions (e.g., detonation of a dirty bomb) (Pandey et al. 2010, Williams et al. 2010). In either scenario, the exposure to high-dose irradiation for a large population underscores the need to have effective mechanisms in place for emergency personnel to cope with mass safety and health concerns. Ideally, the emergency triage response would entail the use of readily accessible bio-fluids (e.g., urine or blood) to screen validated biomarkers for the extent and potential risk to radiation exposure (Blakely et al. 2010, Riecke et al. 2010, Coy et al. 2011). Although there has been considerable effort worldwide from a diverse group of researchers focusing on identifying biomarkers, to date there is still the need to identify and validate readily accessible biomarkers for assessing the extent and predicting injury outcome for exposure to high-dose IR. This is especially true for identifying and treating GI-ARS where mortality onset for humans starts within days of high-dose IR exposure.

One such circulating metabolite that has been identified as a diagnostic biomarker for small intestine function is citrulline (Lutgens et al. 2003, Lutgens et al. 2004). Citrulline is a non-DNA encoded amino acid found in a variety of physiological fluids including blood plasma, urine, cerebrospinal fluid, amniotic fluid, and sweat (Rabier and Kamoun 1995). There are three major metabolic pathways citrulline metabolism is involved in: transformation of ammonia to urea in the liver, synthesis of arginine from glutamine in the GI tract and kidneys, and nitric oxide synthesis (Rabier et al. 1995). The biosynthesis of citrulline originates almost exclusively in small intestinal enterocytes and is maintained at a steady state micromolar concentration in blood circulation (Wu et al. 1994).

A variety of small intestinal conditions including villous atrophy disease (Crenn et al. 2003), Crohn's disease (Papadia et al. 2007), follow-up on small bowel transplantation (Pappas et al. 2001), gut permeability following ethanol exposure (Rendon et al. 2012), and enterocyte functional mass in HIV patients (Cynober et al. 2009) have demonstrated the usefulness of incorporating circulating citrulline concentrations as a functional output for small intestine health. Of particular relevance to GI-ARS, citrulline has been identified as a biomarker for radiation-induced small intestine tissue damage from both chemotherapy (Papadia et al. 2007) and radiotherapy (Lutgens and Lambin 2007). The aforementioned evidence linking citrulline concentration to small intestinal dysfunction and the known association of GI injury to radiation has led to a community-wide suggestion of citrulline as a biomarker for radiation-induced GI tissue damage, although this has not been rigorously evaluated against the GI-ARS time-course.

The use of a plasma citrulline assay for assessing radiation exposure over limited IR doses and time-points in animal models has been carried out in mice (Lutgens et al. 2003, Fu et al. 2009, Garg et al. 2010, Gupta et al. 2011, Jones et al. 2014a, Jones et al. 2014b, Pawar et al. 2014), rats (El-Ghazaly et al. 2015), minipigs (Elliott et al. 2014, Jones et al. 2014b, Moroni et al. 2014b, Shim et al. 2014) and nonhuman primates (NHP) (Hérodin et al. 2012, Jones et al. 2014b). Recently, we reported the link between radiation exposure, plasma citrulline, and small intestine histopathology in a well-characterized murine GI-ARS total-body irradiation

(TBI) model (Jones et al. 2014a). It was shown plasma citrulline levels at day 4 post IR were both dose- and time-dependent, and correlated to small intestine structure/function as measured via histopathology suggesting plasma citrulline was potentially a viable biomarker reflective of GI-ARS at least in a mouse TBI model. Taken together, the clinical and animal model data suggested citrulline was a promising biomarker for diagnosing GI-ARS and had potential value in evaluation of medical countermeasures (MCM). The validation of citrulline as a biomarker for GI-ARS in context of triaging exposed individuals is logistically limited to the use of well-characterized radiation animal models where IR dose and specific time points can be finely tuned in order to systematically account for radiological and temporal variation.

To this end we report the comprehensive characterization of circulating citrulline, small intestine-specific citrulline, and histopathology (images and quantitative measurement of crypt survival) for mice exposed to TBI covering doses of 6 to 15 Gy at consecutive time-points of day 1 to day 6 post IR.

MATERIALS AND METHODS

Radiation Animal Model

Mouse plasma and small intestinal tissue were obtained from Epistem Laboratories Ltd. All mouse procedures were certified according to the UK Animal (Scientific Procedures) Act 1986. Male C57BL/6 mice, aged eight to ten weeks were purchased from Harlan UK and allowed to acclimatize for two weeks prior to irradiation. All mice were held in individually ventilated cages (IVCs) in a specific pathogen free (SPF) barrier unit. There were 5 mice per IVC all from the same treatment group. A twelve hour light:dark cycle was maintained with lights being turned on at approximately 07:00 hours and off at approximately 19:00 hours. There was a constant room temperature of 21 ± 2 °C and a mean relative humidity of 55% ± 10%. The animals received 2918x extruded rodent diet (Harlan) and sterile acidified water (*ad libitum*; pH 2.0–3.0) from time of arrival and throughout the study. Animals were identified by ear punches in cages labeled with the appropriate information necessary to identify the study, dose, animal number, and treatment groups. Animals were irradiated at 15:00 ± one hour (30 animals per radiation dose). Irradiation was performed using an Xstrahl RS320 X-ray set, operated at 300 kV, 10 mA. The X-ray tube had additional filtration to give a radiation quality of 2.3 mm Copper half-value layer (HVL). Mice were restrained in a compartmentalized plexiglass jig, positioned at a distance of 700 mm below the focus of the X-ray tube. Each rectangular box was divided into twelve ventilated restraints, each holding one animal. For this study, ten mice were irradiated simultaneously. A dosimetry device (ion chamber) was placed within the mouse jig to record the dose received to the animals in each run. All radiation doses delivered were within 2.6% of the intended dose (mean 1.9%). Quality assurance and control procedures were performed prior to and during each irradiation to confirm dose and energy output remained within range. Animals received total-body irradiation (TBI) delivered at a dose rate of 81.2 cGy min^{-1}. All animals were weighed and their well-being inspected daily from the initiation of treatment to the end of the study. Mice were humanely euthanized if the weight loss was sustained at greater than 20% for 24 hours and mice also demonstrated signs of a moribund

state (withdrawn behavior, reduced body temperature as judged by feeling cool to touch, lack of grooming and dehydration as judged by a persistent skin tent on pinching). During the peak periods of diarrhea incidence and general decline in well-being, animals were inspected several times during each 24 hour period. On days 1 to 6, five mice per radiation dose were deeply anesthetized with isoflurane and blood collected via cardiac puncture. The mice were then terminated by cervical dislocation. Preparation of mouse plasma was as follows. Blood was collected into 1.5 mL K3 EDTA-coated tubes, immediately placed on wet ice and centrifuged at 5000 g for 5 minutes, at 4 °C within 30 minutes. After centrifugation, the plasma was transferred by sterile pipette into pre-labelled vials and immediately frozen on dry ice. Preparation of mouse intestinal tissue included flushing out contents with PBS. The jejunum was isolated from the small intestine and snap frozen with liquid nitrogen and stored at −80 °C until analyzed for metabolomics.

Quantification of Plasma Citrulline

Plasma citrulline was quantified via liquid chromatography tandem mass spectrometry (LC-MS/MS) as described previously (Jones et al. 2014b). Briefly, 50 uL of plasma spiked with a stable-label internal standard (4,4,5,5-d_4-L-citrulline (d_4-Cit)) was protein precipitated with acetonitrile and analyzed by LC-MS/MS.

Quantification of Jejunal Citrulline

Jejunal citrulline was quantified via liquid chromatography tandem mass spectrometry (LC-MS/MS) using Biocrates AbsoluteIDQ p180 kit (BIOCRATES, Life Science AG, Innsbruck, Austria). The LC-MS/MS platform consisted of a Shimadzu Prominence UFLC XR high-performance liquid chromatograph (HPLC) (Shimadzu, Columbia, MD) coupled to an AB Sciex QTRAP® 5500 hybrid tandem quadrupole/linear ion trap mass spectrometer (AB Sciex, Framingham, MA). The AbsoluteIDQ p180 kit was designed for simultaneous detection and quantification of metabolites from a variety of biological matrices in a high-throughput manner and referred to as high-throughput, targeted metabolomics. The AbsoluteIDQ p180 kit was prepared as described by the manufacturer. Briefly, the kit preparation involved metabolite extraction from the tissue samples by homogenizing in 85:15 (methanol:ethanol, v/v) with 5 mM PBS followed by introduction of stable-label isotope internal standards, amino acid derivatization with 5 % phenylisothiocyanate, and extraction of the metabolites with 5 mM ammonium acetate in methanol on filter inserts of a 96-well plate. Data was analyzed using the MetIQ software (Biocrates, Inc.). Although all metabolites from the AbsoluteIDQ p180 kit were analyzed for, only the citrulline values are presented in this report.

Intestinal Histopathology

Intestinal histopathology was performed using the crypt microcolony assay (Withers and Elkind 1970) on hematoxylin and eosin (H&E) stained slides (Booth et al. 2012, Jones et al. 2014a). The small intestine was removed from each animal and Carnoys fixed. The small intestine was divided into region specific sections: duodenum, jejunum, upper and lower ileum. Each section was “bundled” prior to embedding in order to obtain the ideal orientation of the crypts. From each mouse, a series of small lengths of intestine, approximately 0.5 cm long, were placed within a loop of surgical Micropore tape and the

tape tightened to immobilize the lengths. This allows the alignment of many pieces of fixed intestine alongside each other like a series of logs, so that in every section from a mouse there are several well-orientated cross-sections. Each paraffin block generated was then sectioned to provide one slide per block, each slide containing two non-serial sections, which were stained with H&E. The number of surviving and regenerating crypts per intestinal circumference was scored and the average per mouse and per group determined. A surviving crypt was defined as one that had 10 or more tightly packed strongly H&E stained cells (excluding Paneth cells). Only regions that were orientated correctly and did not contain Peyers patches were scored (Peyers patches influence both the number of crypts in a normal circumference and the ability of a crypt to survive insult). The size of surviving crypts varied, influencing the likelihood of observing a surviving crypt in cross-section, so a size correction factor was applied to reduce this error based on the widths of the crypts (Potten et al. 1981). The corrected number of crypts was calculated according to the following equation: corrected number of crypts = (mean width in control mice / mean width in irradiated mouse) × mean number of surviving crypts in the irradiated mouse. Histopathological analyses were performed on duodenum, jejunum, upper and lower ileum individually. The reported corrected crypt number was the cumulative value of all four tissue sections. Jejunal tissue was shown as a representative example for H&E images.

Statistics

Statistics were calculated for plasma citrulline and jejunal citrulline at each radiation dose level at each study time point. Statistics were also calculated for corrected crypt number at each study time point. Separate simple linear regression models were fit to examine the association of radiation dose level with plasma citrulline, jejunal citrulline, and corrected crypt number at each study time point. Additionally, simple linear regression models were fit to examine the association of corrected crypt number and plasma citrulline level at each study time point. All tests were performed using two-sided tests at the 0.05 significance level. All analyses were performed using SAS (Version 9.4, Copyright © 2014 SAS Institute Inc., Cary, NC) and figures were constructed with GraphPad Prism (v 6.03).

RESULTS

Quantification of plasma citrulline

Plasma citrulline was determined from mice exposed to TBI at exposures of 6 to 15 Gy and at time points of day 1 to day 6 post IR (consecutive days; 14 and 15 Gy did not contain day 6 time points). The mice were sacrificed at designated time points and blood collected via cardiac puncture. There were a total of five mice per time point per IR dose which corresponded to a total of 300 irradiated mice. Non-irradiated control mice were sacrificed with corresponding blood draws at day −7, day 0, and day 6. There were 5 mice per control time point. A total of 315 mice were in the TBI experiment of which plasma was analyzed from 302 mice due to euthanasia criteria of some mice at high-doses at the late time points. Refer to supporting information (SI) Table S1 for tabular representation of the radiological doses, time points, and number of mice. Fig. 1 and Table S2 displayed a line graph and tabulated concentrations, respectively, representing radiological doses temporally across day 1 to day 6 post IR for plasma citrulline for all 302 mice.

To evaluate the response of plasma citrulline following high-dose TBI in the mouse model, linear regression analysis was performed for plasma citrulline versus IR on a per day basis (Table 1 and Fig. S1). There were significant associations between plasma citrulline concentration and radiation dose for each day ($p < 0.0005$ for all days). In other words, higher plasma citrulline concentration was significantly associated with lower levels of IR. However, the best prediction of radiation dose based on the linear regression models were for the later days with days 4, 5 and 6 all having R^2 values greater than 0.71. The slope of the linear regression plot provided an estimate as to the amount of decrease in radiation dose per increase of citrulline. For example, at day 4 there was an estimated decrease of 0.14 Gy per 1 μM increase in plasma citrulline. Refer to Table 1 for estimated IR values per 1 μM increase in plasma citrulline for each day and Fig. 2 for the plot of plasma citrulline concentration versus radiation dose per day.

Another way to visualize the dose response relationship of plasma citrulline on a per day basis was to separate out consecutive IR doses into cohorts that were statistically different (Fig 3). This type of analysis provided the framework to understand at what day post IR, could radiological dose be distinguished based on plasma citrulline. Twenty-four hours (day 1) after the IR event there was no statistical differences between the non-IR plasma citrulline and plasma citrulline from doses 6–15 Gy ($p = 0.86$). By day 2 (48 hours after the IR event) there was clear separation of the lowest IR dose (6 Gy) and control from the higher IR doses ($p < 0.0001$ for both 6 Gy and control to 7–15 Gy). The 6 Gy plasma citrulline value was not statistically different from the control ($p = 0.06$). By day 3, both 6 and 7 Gy plasma citrulline deviated significantly from the 8–15 Gy cohort in addition to being statistically different from each other ($p = 0.008$ for 6 and 7 Gy plasma citrulline on day 3). In comparison to control plasma citrulline, 6 Gy day 3 plasma citrulline was not significantly different ($p = 0.28$) but 7 Gy day 3 plasma citrulline was statistically different ($p = 0.0001$). The trend of each successive day parsing apart more radiological doses based on plasma citrulline held true and by day 5/6 there were 5 to 6 different radiological dose cohorts that were significantly different from each other (Fig 3.).

Quantification of jejunal citrulline

Jejunal citrulline was determined from mice exposed to TBI at exposures of 8, 10, 12, and 14 Gy and at time points of day 1, day 3, and day 5/6 post IR. Jejunum samples at day 6 at 14 Gy were not accessible due to euthanasia criteria and were sampled on day 5. The mice were sacrificed at designated time points and jejunum tissue isolated upon necropsy. Non-irradiated control mice were sacrificed at day −7, day 0, and day 6. There were a total of 4–5 mice per time point per dose. Refer to Table S3 for tabular representation of the radiological doses, time points, and number of mice. Fig. 4 and Table S4 displayed a line graph and tabulated concentrations, respectively, representing radiological doses temporally across days 1, 3, and 5/6 post IR for jejunal citrulline.

In order to compare the citrulline concentration from plasma and jejunum, the absolute concentrations were converted to normalized (%) values. The normalized % was calculated by dividing the absolute concentration by the mean concentration of the control (non-IR) samples. Plots of the normalized citrulline concentration for plasma and jejunum versus the

day post IR for 8, 10, 12, and 14 Gy were displayed in Fig. 5. In addition, linear regression analysis was performed for each radiological dose (Fig. S2). The R^2 values were 0.98 (8 Gy), 0.99 (10 Gy), 0.99 (12 Gy), and 0.99 (14 Gy) which demonstrated a significant linear correlation across radiological and temporal variation between plasma and jejunal citrulline. In effect, plasma citrulline directly corresponded to jejunal citrulline and the use of plasma citrulline as a surrogate for small intestinal citrulline was valid.

Small intestinal histopathology: H&E staining and crypt survival determination

Sections of the small intestine were collected and investigated via H&E staining for evaluation of the structural integrity of the small intestine and for quantitative determination of crypt survival by corrected crypt number (CCN) calculations. The H&E images of jejunal tissue from non-irradiated control and IR doses 6, 8, 10, 12, and 14 Gy spanning days 2, 4, and 5/6 detailed the pathology of the small intestine in the mouse model following exposure to high-dose IR (Fig. 6). The normal non-irradiated jejunum tissue was characterized by a well-defined mucosal barrier lined with crypt-to-villus fine structure. Radiation compromised the crypt clonogenic cells which in turn diminished cellular output onto the villi leading to impaired cell production and gradual deterioration of the crypt-to-villus architecture. The extent of the mucosal damage and degree of recovery was dose and time dependent. At the lower, sub GI-ARS, radiation doses (6–9 Gy) where tissue damage was minimal (since crypt clonogenic cells were not entirely obliterated) and GI injury was not associated with intestinal ulceration or diarrhea (Booth et al. 2012), transient interruption of cell proliferation was present and triggered regenerative epithelial hyperplasia as evident by the increased number of differentiated functional upper crypt and villus cells which in turn increase the size of these structures.

The mid-range TBI doses of 10–12 Gy were associated by noticeable loss of epithelium (moderate to heavy villus blunting) due to substantial killing of crypt cells. By day 6, the rapid regeneration from the surviving crypt cells restored a functional albeit still recovering epithelium. The higher TBI doses (13–15 Gy) which corresponded to lethal GI-ARS were characterized by widespread loss of functional clonogenic cells as evident by severe villus blunting with corresponding extensive deterioration of the epithelial layer, resulting in ulceration and submucosal inflammation. The rapid regeneration of the intact epithelial barrier seen in the lower TBI doses was not evident in the GI lethal doses. Therefore recovery of the mucosal structure and function was minimal.

The CCN for the small intestine was determined from mice exposed to TBI 6 to 15 Gy and at time points of day 1 to day 6 post IR (consecutive days; 14 and 15 Gy did not contain day 6 time points). The numbers of mice and time points corresponded to the data presented for the plasma citrulline. Fig. 7 and Table S5 displayed a line graph and tabulated values, respectively, representing radiation doses temporally across day 1 to day 6 post IR for CCN values for all mice.

To evaluate the response of CCN to high-dose TBI in the mouse model, linear regression analysis was performed for CCN versus irradiation on a per day basis (Table 2 and Fig. S3). There were significant associations between CCN values and irradiation dose for each day where higher CCN values were significantly associated with lower levels of irradiation

(p<0.0003 for all days). The linear regression analysis yielded R^2 values greater than 0.88 for all days excluding day 1 indicating a robust linear fit for predicting IR dose based on CCN for days 2 through 6 over IR doses of 6–15 Gy. The slope of the linear regression plots provided an estimate as to the amount of decrease in radiation dose per increase of CCN. For example, at day 2 there was an estimated decrease of 0.88 Gy per 10 unit increase in CCN. Refer to Table 2 for estimated IR values per increase in CCN for each day and Fig. 8 for the plot of CCN values versus IR dose per day.

Statistical correlation between plasma citrulline and intestinal histopatholgy

The correlation between plasma citrulline and intestinal histopatholgy as measured by CCN was evaluated temporally per dose and radiologically per day. The temporal comparison via linear regression demonstrated significant associations (p <0.0013 for all doses) between plasma citrulline and CCN per dose over the time course of day 1 to day 6 (Table 3 and Fig. S4). The linear fit for the relationship between plasma citrulline and CCN resulted in R^2 values greater than 0.75 for IR doses 9 Gy and higher except for 10 Gy which had a R^2 value of 0.59. The linear relationship at the lower IR doses (6, 7, and 8 Gy) was less ideal with R^2 values less than 0.34. The robust linear fit between temporal variation of plasma citrulline and CNN for IR doses 9 Gy and higher provided a model for predicting CCN based on plasma citrulline. Refer to Fig. 9 for the plot of normalized plasma citrulline and CCN versus day per IR dose. The normalized values were computed using the mean values for the control samples analogous to Fig. 5.

To evaluate the comparison of plasma citrulline to CCN per day by IR dose in the mouse TBI model, linear regression analysis was performed for plasma citrulline versus CCN per day (Table 4 and Fig. S5). There were significant associations (p <0.0001) between plasma citrulline and CCN for each day except for day 1 which was not significantly associated (p =0.37). For days 2 through 6, higher plasma citrulline was significantly associated with higher CCN values. However, the best predictions of IR dose based on the linear regression models were for days 3, 4, and 5 all having R^2 values greater than 0.70. The slope of the linear regression plot provided an estimate as to the amount of increase in CCN per increase of citrulline. For example, at day 3 there was an estimated increase of 3.02 in CCN per 1 μM increase in plasma citrulline. Refer to Table 4 for estimated CCN values per 1 μM increase in plasma citrulline for each day and Fig. 10 for the plot of plasma citrulline versus CCN per day.

DISCUSSION

The use of plasma citrulline as a biomarker, specifically as it relates to GI-ARS, has been described previously using mouse, rat, minipig, and NHP radiation models (Lutgens et al. 2003, Fu et al. 2009, Garg et al. 2010, Gupta et al. 2011, Hérodin et al. 2012, Elliott et al. 2014, Pawar et al. 2014, Shim et al. 2014, Jones et al. 2014a, Jones et al. 2014b, Moroni et al. 2014a, El-Ghazaly et al. 2015). Lutgens et al (2003) using a TBI mouse model reported plasma citrulline concentration kinetics were dose-dependent and plasma citrulline levels were correlated to mucosal surface lining. It was concluded plasma citrulline was a simple and sensitive marker for monitoring small bowel epithelial damage following high-dose

irradiation. Similar results from comparable dosing schedules and time points covering mice, rat, minipig, and NHP radiation models from the references mentioned above further substantiated the link between plasma citrulline, radiation effects over time, and small intestine injury.

The present data-set described herein not only extended but provided fundamental insight into the relationship between plasma citrulline, small intestinal citrulline, and small intestinal epithelial damage and recovery (as measured by crypt survival) in the mouse TBI model covering radiation dose ranges of non-lethal to lethal GI-ARS. The experimental parameters provided a robust analysis of plasma citrulline, jejunal citrulline, and small intestinal crypt survival from mice exposed to TBI 6 to 15 Gy over time points from day 1 to day 6 post IR. The consecutive time points of days 1 to 6 covered small intestine epithelial cell cycle turnover following high-dose irradiation. The small intestine epithelium is acutely prone to radiation and is characterized by dose-dependent mucosal damage and subsequent dose-dependent regeneration from surviving clonogenic cells (Booth and Potten 2002).

Plasma citrulline from non-irradiated (naïve) mice were sampled over a two week time period (days −7, 0, and 6 in relation to the IR event) in order to assess the temporal profile of control mouse plasma citrulline. There were no significant differences between plasma citrulline sampled over the two week time period and the mean value for 15 individual mice was determined to be 39.2 ± 1.7 μM. This value was in agreement with reported literature not only in other mouse models (Brown et al. 2011, Gupta et al. 2011, Jaisson et al. 2012, Jones et al. 2014b) but also in NHP models (39.3 ± 1.3 μM) (Jones et al. 2014b; Jones et al 2015) and human studies (40 ± 10 μM) (Rabier et al. 1995, Crenn et al. 2008, Demacker et al. 2009, Brown et al. 2011). The results indicated that plasma citrulline in the mouse model was a comparable surrogate for large animal models and humans.

Higher plasma citrulline values were significantly associated with lower IR doses across all days with days 4, 5 and 6 providing the best linear fit. In other words, plasma citrulline displayed a dose-dependent response across the temporal profile with potential prediction of the radiation dose if the day post IR was known. Although clonogen death occurs on day 1 following IR exposure, the consequences of clonogen death peak at day 3 (Potten and Booth 1997). In this regards, day 1 was not informative for determining IR dose based on plasma citrulline. Day 2 and 3 post IR plasma citrulline concentrations statistically distinguished the lower IR doses of 6 and 7 Gy from the higher doses (8–15 Gy). The ability based on plasma citrulline to tease apart IR doses associated with hematopoietic (H)-ARS (6 and 7 Gy) from IR doses more closely aligned with GI-ARS (8–15 Gy) within 48 to 72 hours of the irradiation event highlighted the potential role plasma citrulline in the mouse model has in predicting radiation injury. Although not statistically significant, 6 Gy plasma citrulline values at day 2 and 3 decreased relative to the mean control values. By day 4, plasma citrulline values for the 6 Gy IR dose exceeded control values and continued to increase out to day 6. The plasma citrulline levels for 6 Gy on days 4–6 compared to control values all reached significance (p <0.0001 for days 4, 5 and 6). The elevated plasma citrulline levels at days 4–6 for 6 Gy indicated the IR event although not particularly disruptive to plasma citrulline over days 1–3 did affect small intestine epithelial cell proliferation homeostasis. The only other IR dose to reach mean control plasma citrulline values was 7 Gy which

returned to control levels by day 4 (p =0.99 for 7 Gy day 4 and control). Moreover, plasma citrulline values for 7 Gy at days 5 and 6 remained similar to control values (p >0.13) unlike plasma citrulline values for 6 Gy at days 5 and 6.

The link between plasma citrulline and small intestine enterocyte mass is well documented (Wakabayashi et al. 1991, Wakabayashi et al. 1995) but the direct comparison of plasma citrulline to small intestinal citrulline has not been well characterized in radiation animal models. Citrulline from jejunal tissue that was matched to plasma citrulline from the same mouse was determined for non-irradiated controls over a two week window (three time points at day −7, 0, and 6 in relation to the IR event) and from IR doses ranging from 8–14 Gy at time points out to day 6. The statistical analysis demonstrated plasma and jejunal citrulline have a robust linear correlation and the use of plasma citrulline to inform on small intestine citrulline was valid. These results further substantiated the dose-response relationship of small intestine enterocyte mass and plasma citrulline.

Morphologic endpoints such as the use of histopathology to visualize the structural integrity of the small intestine have been the benchmark for assessing GI-ARS (Potten et al. 1997). H&E images of the TBI mouse model demonstrated radiation killed the crypt clonogenic cells and with successive loss of clonogens the cellular output onto the villi was drastically impacted resulting in dose- and time-dependent tissue damage to the mucosal layer of the small intestine. Tissue damage was evident by day 2 across the IR doses and subsequent recovery or continued impairment was observed in a dose-dependent fashion out to day 6. CCN values were calculated for the collective small intestine (duodenum, jejunum, and ileum) as a quantitative measurement of crypt survival and structural integrity of the small intestine mucosal fine structure. Higher CCN values were significantly associated with lower IR dose with days 2 through 6 all providing robust linear fits indicating the CCN was highly informative for describing the impact radiation has in small intestine crypt survival and corresponding structural health. The comprehensive collection of CCN for the mouse TBI model (6–15 Gy) over consecutive time points of 1 to 6 days post IR has not been reported previously. The lower IR doses of 6 and 7 Gy displayed similar temporal profiles and reached near control values by day 6 (reaching 93 % of control CCN values for both 6 and 7 Gy). All other IR doses failed to reach control CCN values over the 6 day time period with 8–9 Gy obtaining 58–71 % recovery, 10–11 Gy reaching 25–34 % recovery, 12–13 Gy reaching 12–16 % recovery, and 14–15 Gy (measured at day 5) at near complete loss of all crypts (1–2 % of control CCN values).

The comparison of the plasma citrulline to CCN provided the framework for evaluating plasma citrulline’s role not just as a marker of enterocyte mass, but its role in characterizing structural damage and recovery of the small intestine upon radiation-induced injury. Higher plasma citrulline was significantly associated with higher CCN for both radiological and temporal variation. The linear correlation was poor for the low doses (6, 7, and 8 Gy) when considering temporal variation but the linear model yielded a more consistent fit for the higher doses (9–15 Gy). The results suggested plasma citrulline was a marker for clonogen damage associated epithelial loss and regeneration, but was less adequate for H-ARS when the effects on mucosal mass were minimal. There was no correlation between plasma citrulline and CCN on day 1 following IR. On the other hand, plasma citrulline values were

significantly associated with higher CCN values for days 2–6 with days 3, 4, and 5 providing the best linear fit.

Considering the breadth of the plasma citrulline and crypt survival data collected from the mouse TBI model including the initial and early time points of the GI-ARS injury, the data presented herein further delineated plasma citrulline's role as a biomarker for GI injury from high-dose irradiation. The data not only displayed a strong correlation between plasma citrulline concentration and dose-response it also emphasized the relationship between plasma citrulline and GI-ARS including notable limitations when associating plasma citrulline to characterize GI-ARS. The utility of plasma citrulline was realized in the context of using a well-characterized animal model where the relationship between radiation dose and GI-ARS incidence, timing, and severity were established and correlated to histopathology. The use of plasma citrulline as a single biomarker of GI injury resulting from high-dose irradiation was limited in its scope. However, its continued use in the framework of a well-characterized animal model where fundamental understanding of the GI injury are understood will prove to be advantageous in providing insight towards GI-ARS in terms of injury and recovery.

CONCLUSION

The use of plasma citrulline as a biomarker to characterize GI-ARS in the murine TBI model was evaluated in the context of matching small intestinal citrulline and histopathology. To date, the data set represented the more comprehensive attempt in terms of radiation doses and time points post exposure to understand plasma citrulline and its role in characterizing GI-ARS in the mouse model. Plasma citrulline was significantly associated with small intestinal citrulline levels as measured in the jejunum for both radiological and temporal variation following TBI. In addition, plasma citrulline was significantly associated with crypt survival (as measured via corrected crypt number) with the best correlation arising from TBI doses of 9–15 Gy over days 2–5 post irradiation. The data suggested plasma citrulline was indeed an informative marker for assessing GI injury following high-dose irradiation.

Supplementary Material

Refer to Web version on PubMed Central for supplementary material.

Acknowledgments

This project has been funded in whole or in part with Federal funds from the National Institute of Allergy and Infectious Diseases, National Institutes of Health, Department of Health and Human Services, under Contract No. HHSN272201000046C. Additional support was provided by the University of Maryland School of Pharmacy Mass Spectrometry Center (SOP1841-IQB2014). The authors would like to thank all members of the Medical Countermeasures Against Radiological Threats (MCART) consortium for their dedication, support, and guidance in establishing biomarker identification and validation as a priority in the radiation medical counter measure field. Additionally, we would like to acknowledge and thank all members of the Kane laboratory.

References

Blakely WF, Ossetrova NI, Whitnall MH, Sandgren DJ, Krivokrysenko VI, Shakhov A, Feinstein E. Multiple parameter radiation injury assessment using a nonhuman primate radiation model-biodosimetry applications. Health Phys. 2010; 98:153–159.10.1097/HP.0b013e3181b0306d [PubMed: 20065677]

Booth, C.; Potten, CS. The Intestine as a Model for Studying Stem-Cell Behavior. In: Teicher, B., editor. Tumor Models in Cancer Research. Humana Press; Totawa: 2002. p. 337-357.

Booth C, Tudor G, Tudor J, Katz BP, MacVittie TJ. Acute Gastrointestinal Syndrome in High-Dose Irradiated Mice. Health Phys. 2012; 103:383–399.10.1097/HP.0b013e318266ee13 [PubMed: 23091876]

Brown CM, Becker JO, Wise PM, Hoofnagle AN. Simultaneous determination of 6 L-arginine metabolites in human and mouse plasma by using hydrophilic-interaction chromatography and electrospray tandem mass spectrometry. Clin Chem. 2011; 57:701–709.10.1373/clinchem.2010.155895 [PubMed: 21406573]

Coy SL, Cheema AK, Tyburski JB, Laiakis EC, Collins SP, Fornace A. Radiation metabolomics and its potential in biodosimetry. Int J Radiat Biol. 2011; 87:802–823.10.3109/09553002.2011.556177 [PubMed: 21692691]

Crenn P, Messing B, Cynober L. Citrulline as a biomarker of intestinal failure due to enterocyte mass reduction. Clin Nutr. 2008; 27:328–339.10.1016/j.clnu.2008.02.005 [PubMed: 18440672]

Crenn P, Vahedi K, Lavergne-Slove A, Cynober L, Matuchansky C, Messing B. Plasma citrulline: a marker of enterocyte mass in villous atrophy-associated small bowel disease. Gastroenterology. 2003; 124:1210–1219.10.1016/S0016-5085(03)00170-7 [PubMed: 12730862]

Cynober L, Melchior JC, Crenn P, De Truchis P, Neveux N, Galpe T. Plasma citrulline is a biomarker of enterocyte mass and an indicator of parenteral nutrition in HIV-infected patients. Am J Clin Nutr. 2009; 90:587–594. [PubMed: 19587086]

Demacker PNM, Beijers AM, van Daal H, Donnelly JP, Blijlevens NMA, van den Ouweland JMW. Plasma citrulline measurement using UPLC tandem mass-spectrometry to determine small intestinal enterocyte pathology. J Chromatogr B. 2009; 877:387–392.

El-Ghazaly MA, El-Hazek RM, Khayyal MT. Protective effect of the herbal preparation, STW 5, against intestinal damage induced by gamma radiation in rats. Int J Radiat Biol. 2015; 91:150–156.10.3109/09553002.2014.954059 [PubMed: 25131937]

Elliott TB, Deutz NE, Gulani J, Koch A, Olsen CH, Christensen C, Chappell M, Whitnall MH, Moroni M. Gastrointestinal acute radiation syndrome in Göttingen minipigs (Sus scrofa domestica). Comp Med. 2014; 64:456–463. [PubMed: 25527026]

Fu Q, Berbée M, Boerma M, Wang J, Schmid HA, Hauer-Jensen M. The somatostatin analog SOM230 (pasireotide) ameliorates injury of the intestinal mucosa and increases survival after total-body irradiation by inhibiting exocrine pancreatic secretion. Radiat Res. 2009; 171:698–707.10.1667/RR1685.1 [PubMed: 19580476]

Garg S, Boerma M, Wang J, Fu Q, Loose DS, Kumar KS, Hauer-Jensen M. Influence of Sublethal Total-Body Irradiation on Immune Cell Populations in the Intestinal Mucosa. Radiat Res. 2010; 173:469–478.10.1667/RR1742.1 [PubMed: 20334519]

Gupta PK, Brown J, Biju PG, Thaden J, Deutz NE, Kumar S, Hauer-Jensen M, Hendrickson HP. Development of high-throughput HILIC-MS/MS methodology for plasma citrulline determination in multiple species. Anal Methods. 2011; 3:1759–1768.10.1039/c1ay05213f

Hérodin F, Richard S, Grenier N, Arvers P, Gérome P, Baugé S, Denis J, Chaussard H, Gouard S, Mayol J-F, Agay D, Drouet M. Assessment of total- and partial-body irradiation in a baboon model: preliminary results of a kinetic study including clinical, physical, and biological parameters. Health Phys. 2012; 103:143–149. [PubMed: 22951472]

Jaisson S, Gorisse L, Pietrement C, Gillery P. Quantification of plasma homocitrulline using hydrophilic interaction liquid chromatography (HILIC) coupled to tandem mass spectrometry. Anal Bioanal Chem. 2012; 402:1635–1641. [PubMed: 22160237]

Jones JW, Scott AJ, Tudor G, Xu P-T, Jackson IL, Vujaskovic Z, Booth C, MacVittie TJ, Ernst RK, Kane MA. Identification and Quantitation of Biomarkers for Radiation-induced Injury via Mass Spectrometry. Health Phys. 2014; 106:106–119. [PubMed: 24276554]

Jones JW, Tudor G, Bennett A, Farese AM, Moroni M, Booth C, MacVittie TJ, Kane MA. Development and validation of a LC-MS/MS assay for quantitation of plasma citrulline for application to animal models of the acute radiation syndrome across multiple species. Anal Bioanal Chem. 2014; 406:4663–4675. [PubMed: 24842404]

Lutgens LC, Lambin P. Biomarkers for radiation-induced small bowel epithelial damage: an emerging role for plasma Citrulline. World J Gastroenterol. 2007; 13:3033–3042. [PubMed: 17589917]

Lutgens LC, Deutz NE, Gueulette J, Cleutjens JP, Berger MP, Wouters BG, von Meyenfeldt MF, Lambin P. Citrulline: A physiologic marker enabling quantitation and monitoring of epithelial radiation-induced small bowel damage. Int J Radiat Oncol. 2003; 57:1067–1074.

Lutgens LC, Deutz N, Granzier-Peeters M, Beets-Tan R, De Ruysscher D, Gueulette J, Cleutjens J, Berger M, Wouters B, von Meyenfeldt M, Lambin P. Plasma citrulline concentration: a surrogate end point for radiation-induced mucosal atrophy of the small bowel. A feasibility study in 23 patients. Int J Radiat Oncol Biol Phys. 2004; 60:275–285. [PubMed: 15337566]

Moroni M, Elliott TB, Deutz NE, Olsen CH, Owens R, Christensen C, Lombardini ED, Whitnall MH. Accelerated hematopoietic syndrome after radiation doses bridging hematopoietic (H-ARS) and gastrointestinal (GI-ARS) acute radiation syndrome: early hematological changes and systemic inflammatory response syndrome in minipig. Int J Radiat Biol. 2014; 90:363–372.10.3109/09553002.2014.892226 [PubMed: 24524283]

Moroni M, Port M, Koch A, Gulani J, Meineke V, Abend M. Significance of bioindicators to predict survival in irradiated minipigs. Health Phys. 2014; 106:727–733. [PubMed: 24776906]

Pandey BN, Kumar A, Tiwari P, Mishra KP. Radiobiological basis in management of accidental radiation exposure. Int J Radiat Biol. 2010; 86:613–635. [PubMed: 20673129]

Papadia C, Sherwood RA, Kalantzis C, Wallis K, Volta U, Fiorini E, Forbes A. Plasma citrulline concentration: a reliable marker of small bowel absorptive capacity independent of intestinal inflammation. Am J Gastroenterol. 2007; 102:1474–1482. [PubMed: 17459021]

Pappas PA, Saudubray JM, Tzakis AG, Rabier D, Carreno MR, Gomez-Marin O, Huijing F, Gelman B, Levi DM, Nery JR, Kato T, Mittal N, Nishida S, Thompson JF, Ruiz P. Serum citrulline and rejection in small bowel transplantation: a preliminary report. Transplantation. 2001; 72:1212–1216. [PubMed: 11602844]

Pawar SA, Shao L, Chang J, Wang W, Pathak R, Zhu X, Wang J, Hendrickson H, Boerma M, Sterneck E, Zhou D, Hauer-Jensen M. C/EBPδ deficiency sensitizes mice to ionizing radiation-induced hematopoietic and intestinal injury. PLoS One. 2014; 9:e94967. [PubMed: 24747529]

Potten CS, Booth C. The role of radiation-induced and spontaneous apoptosis in the homeostasis of the gastrointestinal epithelium: a brief review. Comp Biochem Physiol B Biochem Mol Biol. 1997; 118:473–478. [PubMed: 9467859]

Potten CS, Rezvani M, Hendry JH, Moore JV, Major D. The correction of intestinal microcolony counts for variation in size. Int J Radiat Biol Relat Stud Phys Chem Med. 1981; 40:321–326. [PubMed: 7026475]

Rabier D, Kamoun P. Metabolism of citrulline in man. Amino Acids. 1995; 9:299–316.10.1007/BF00807268 [PubMed: 24178879]

Rendon JL, Li X, Gupta P, Hauer-Jensen M, Choudhry MA. Decreased serum citrulline correlates with increased gut permeability following ethanol exposure and burn injury. Alcohol. 2012; 42:177.

Riecke A, Ruf CG, Meineke V. Assessment of radiation damage-the need for a multiparametric and integrative approach with the help of both clinical and biological dosimetry. Health Phys. 2010; 98:160–167.10.1097/HP.0b013e3181b97306 [PubMed: 20065678]

Shim S, Jang W-S, Lee S-J, Jin S, Kim J, Lee S-S, Bang HY, Jeon BS, Park S. Development of a new minipig model to study radiation-induced gastrointestinal syndrome and its application in clinical research. Radiat Res. 2014; 181:387–395. [PubMed: 24786169]

Wakabayashi Y, Yamada E, Hasegawa T, Yamada R. Enzymological evidence for the indispensability of small intestine in the synthesis of arginine from glutamate. Arch Biochem Biophys. 1991; 291:1–8.10.1016/0003-9861(91)90097-3 [PubMed: 1929423]

Wakabayashi Y, Yamada E, Yoshida T, Takahashi N. Effect of intestinal resection and arginine-free diet on rat physiology Effect of intestinal on rat physiology resection and arginine-free diet. Am J Physiol Gastrointest Liver Physiol. 1995; 269:G313–G318.

Williams JP, Brown SL, Georges GE, Hauer-Jensen M, Hill RP, Huser AK, Kirsch DG, Macvittie TJ, Mason KA, Medhora MM, Moulder JE, Okunieff P, Otterson MF, Robbins ME, Smathers JB, McBride WH. Animal models for medical countermeasures to radiation exposure. Radiat Res. 2010; 173:557–578.10.1667/RR1880.1 [PubMed: 20334528]

Withers HR, Elkind MM. Microcolony survival assay for cells of mouse intestinal mucosa exposed to radiation. Int J Radiat Biol Relat Stud Phys Chem Med. 1970; 17:261–267. [PubMed: 4912514]

Wu G, Knabe DA, Flynn NE. Synthesis of citrulline from glutamine in pig enterocytes. Biochem J. 1994; 299:115–21. [PubMed: 8166628]

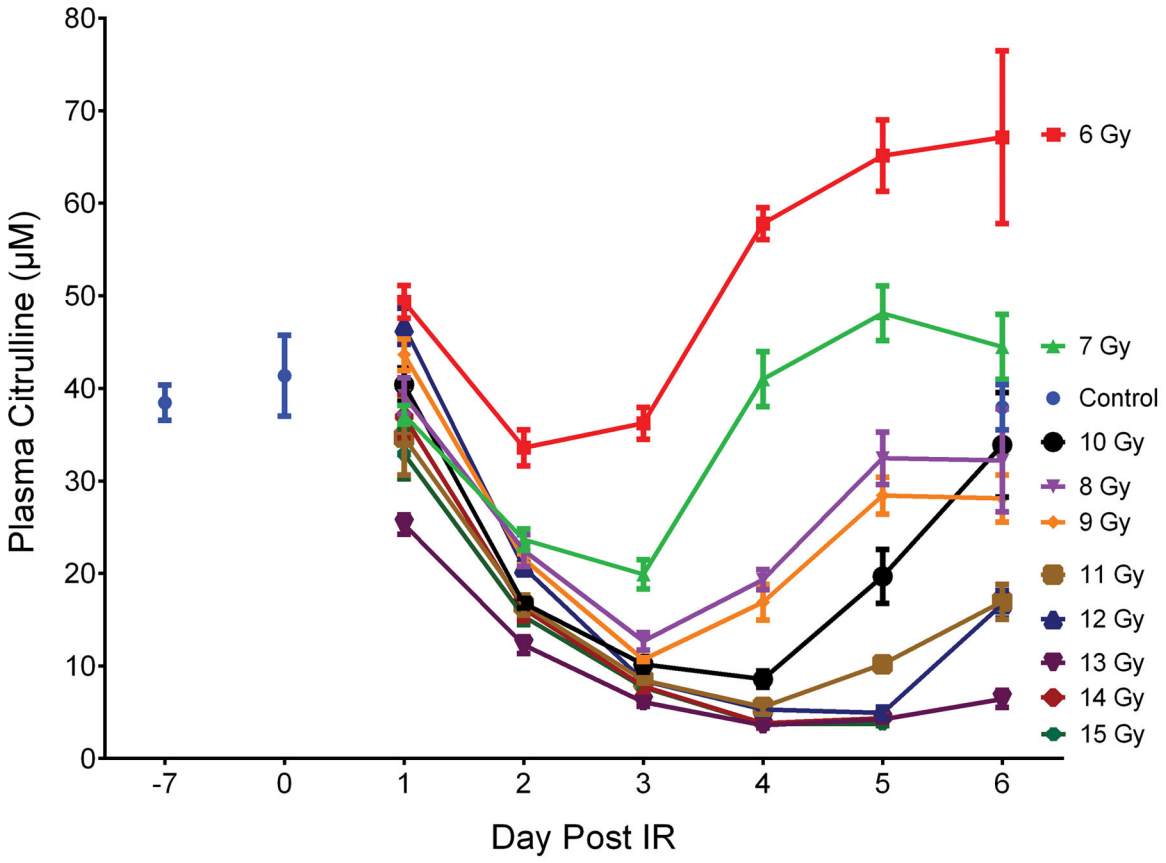

Fig. 1.

Plasma citrulline expressed as a function of day post IR. Day −7 corresponded to plasma samples from age-matched non-irradiated control mice 7 days prior to IR. Day 0 corresponded to plasma samples from age-matched non-irradiated control mice just prior to IR. Plasma samples for day 6 at 14 and 15 Gy were not accessible due to euthanasia criteria and were sampled on day 5. Concentrations were expressed in μM as mean ± sem. Refer to Table S2 for tabulated values for concentrations, error, and number of independent plasma samples.

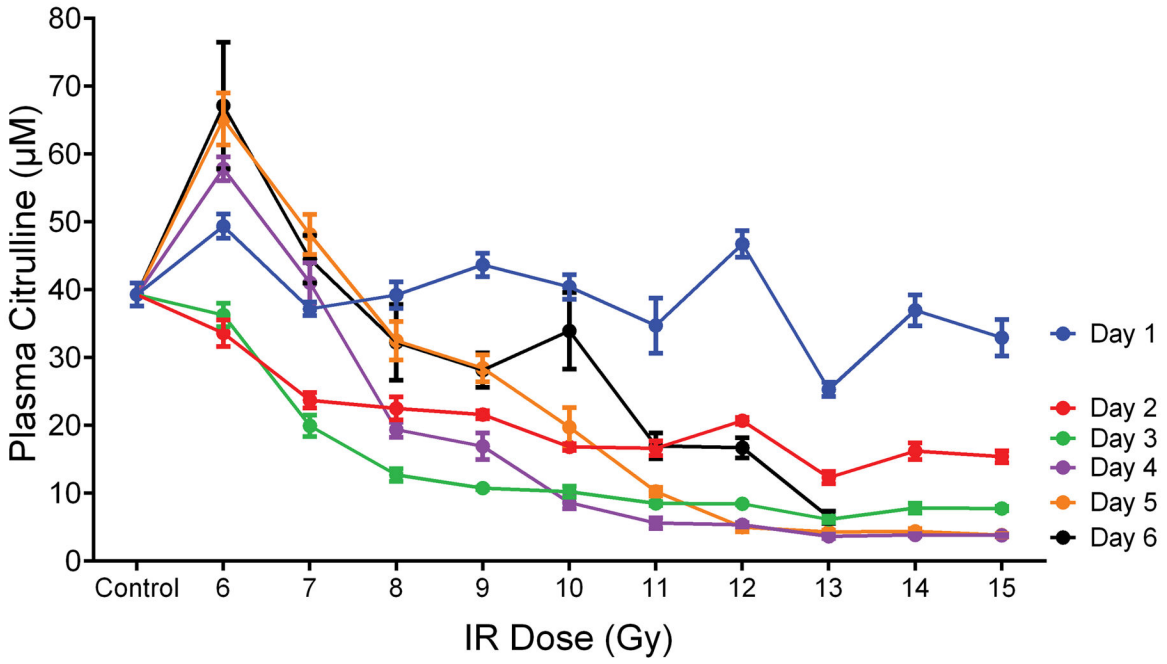

Fig. 2.

Plasma citrulline expressed as a function of IR dose per day. Control was the mean of plasma samples from all control time points (day −7, day 0 and day 6; n=15). Plasma samples for day 6 at 14 and 15 Gy were not accessible due to euthanasia criteria and were sampled on day 5. Concentrations were expressed in μM as mean ± sem.

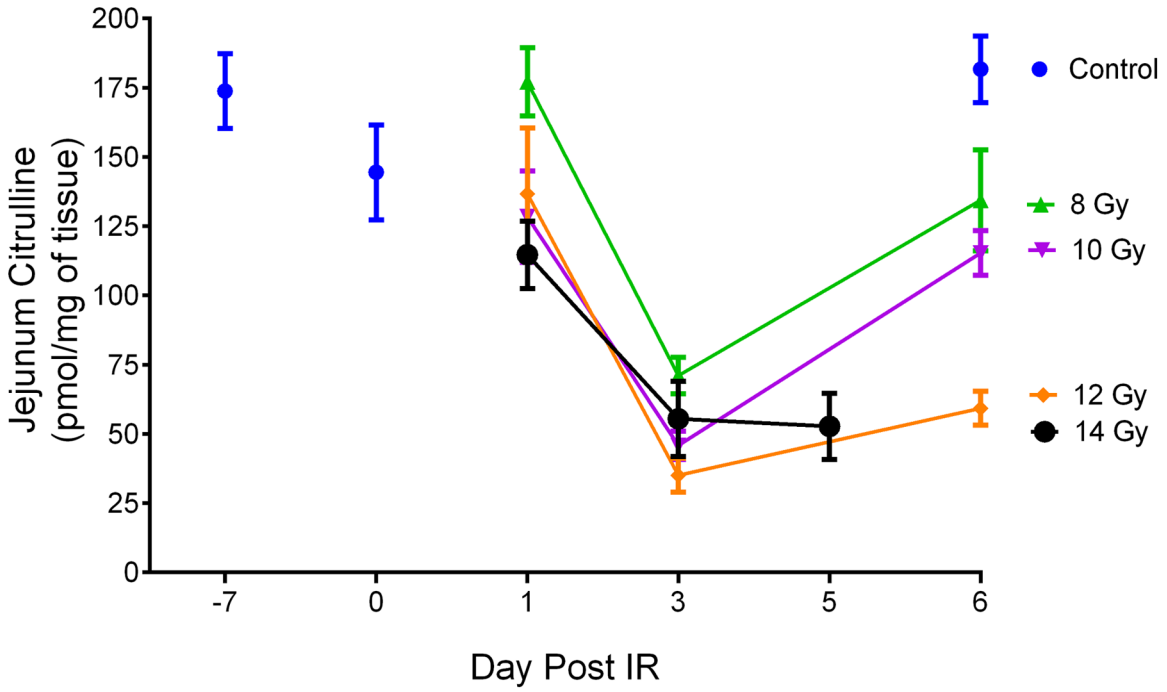

Fig. 3.

Plasma citrulline expressed as a function of IR dose per Day. The IR dose was separated into cohorts based on consecutive IR doses being significantly different. A.) Day 1 post IR comparing control (non-irradiated) to all IR doses (6–15 Gy). There was no significant difference between the two groups ($p = 0.86$). B.) Day 2 post IR comparing control, 6 Gy and 7–15 Gy. There was no significant difference between the control and 6 Gy ($p = 0.06$). There was significant difference between 6 and 7–15 Gy ($p < 0.0001$). C.) Day 3 post IR comparing control, 6 Gy, 7 Gy, and 8–15 Gy. There was no significant difference between the control and 6 Gy ($p = 0.28$). There were significant differences between 6 and 7 Gy ($p = 0.008$), and 7 and 8–15 Gy ($p < 0.0001$). D.) Day 4 post IR comparing control, 6 Gy, 7 Gy, 8–9 Gy and 10–15 Gy. There was no significant difference between the control and 7 Gy ($p = 0.56$). There were significant differences between control and 6 Gy ($p = 0.0001$), 6 and 7 Gy ($p = 0.008$), 7 and 8–9 Gy ($p = 0.0007$), and 8–9 Gy and 10–15 Gy ($p < 0.0001$). E.) Day 5 post-IR comparing control, 6 Gy, 7 Gy, 8–9 Gy, 10 Gy, 11 Gy, and 12–15 Gy. There were significant differences between control and 6 Gy ($p = 0.0001$), 6 and 7 Gy ($p = 0.016$), 7 and 8–9 Gy ($p = 0.0007$), 8–9 Gy and 10 Gy ($p = 0.014$), 10 Gy and 11 Gy ($p = 0.016$), and 11 Gy and 12–15 Gy ($p = 0.0002$). F.) Day 6 post-IR comparing control, 6 Gy, 7 Gy, 8–10 Gy, 11–12 Gy, and 13–15 Gy. There were significant differences between control and 6 Gy ($p = 0.0003$), 6 and 7 Gy ($p = 0.032$), 7 and 8–9 Gy ($p = 0.033$), 8–10 Gy and 11–12 Gy ($p < 0.0001$), and 11–12 Gy and 13–15 Gy ($p < 0.0001$). All values were reported in μM as mean ± sem. * = $p < 0.05$, **= $p < 0.01$, ***= $p < 0.005$, ****= $p < 0.0001$.

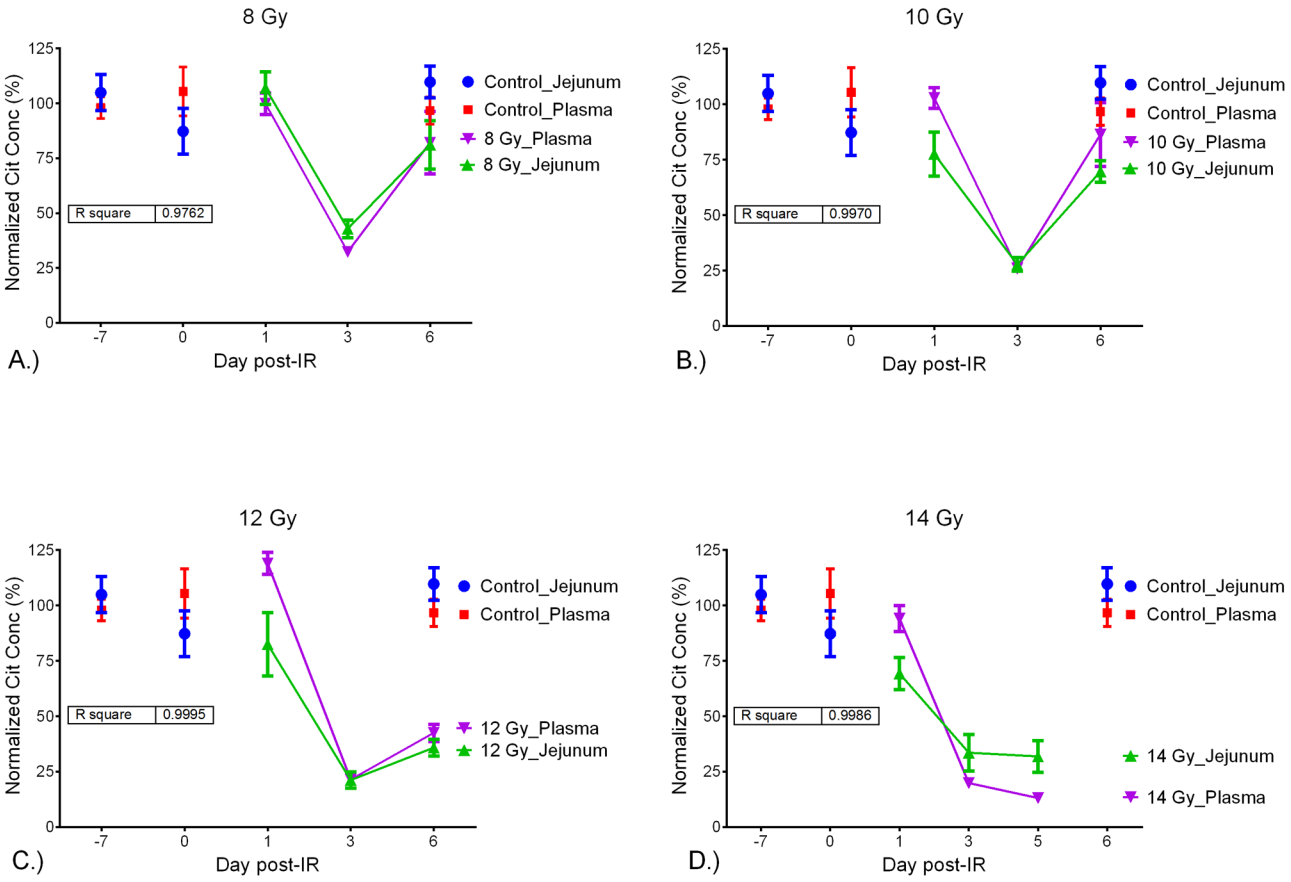

Fig. 4.

Jejunal citrulline expressed as a function of day per IR dose. Day −7 corresponded to tissue samples from age-matched non-irradiated control mice 7 days prior to IR. Day 0 corresponded to tissue samples from age-matched non-irradiated control mice just prior to IR. Jejunal samples for day 6 at 14 Gy were not accessible due to euthanasia criteria and were sampled on day 5. Concentrations were expressed in pmol/mg of tissue as mean ± sem. Refer to Table S4 for tabulated values for concentrations, error, and number of independent tissue samples.

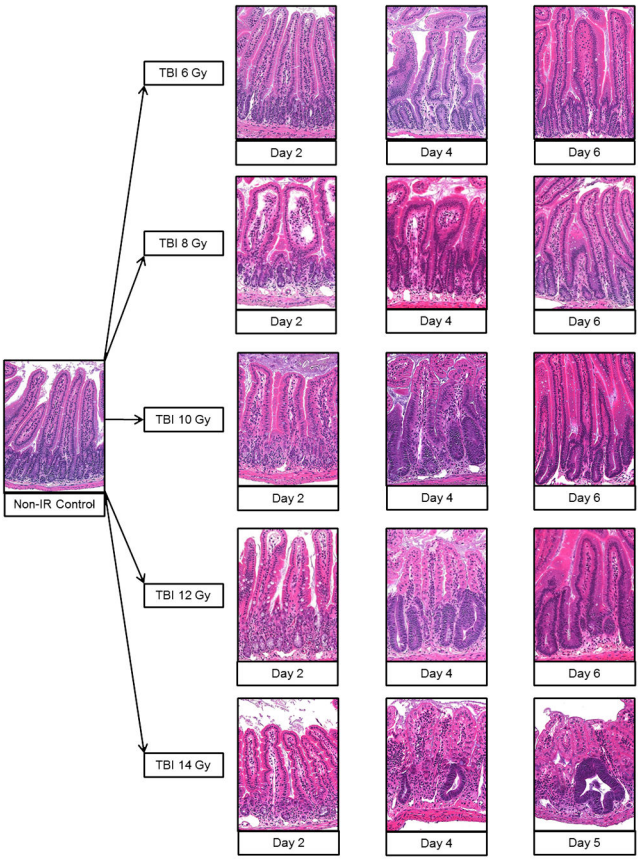

Fig. 5.

Normalized (%) values for jejunal and plasma citrulline versus the day post-IR. Plot shows jejunal and plasma citrulline at IR dose versus the day post IR. Inset displays R^2 generated via linear regression analysis comparing jejunal and plasma citrulline. A.) 8 Gy, B.) 10 Gy, C.) 12 Gy, D.) 14 Gy.

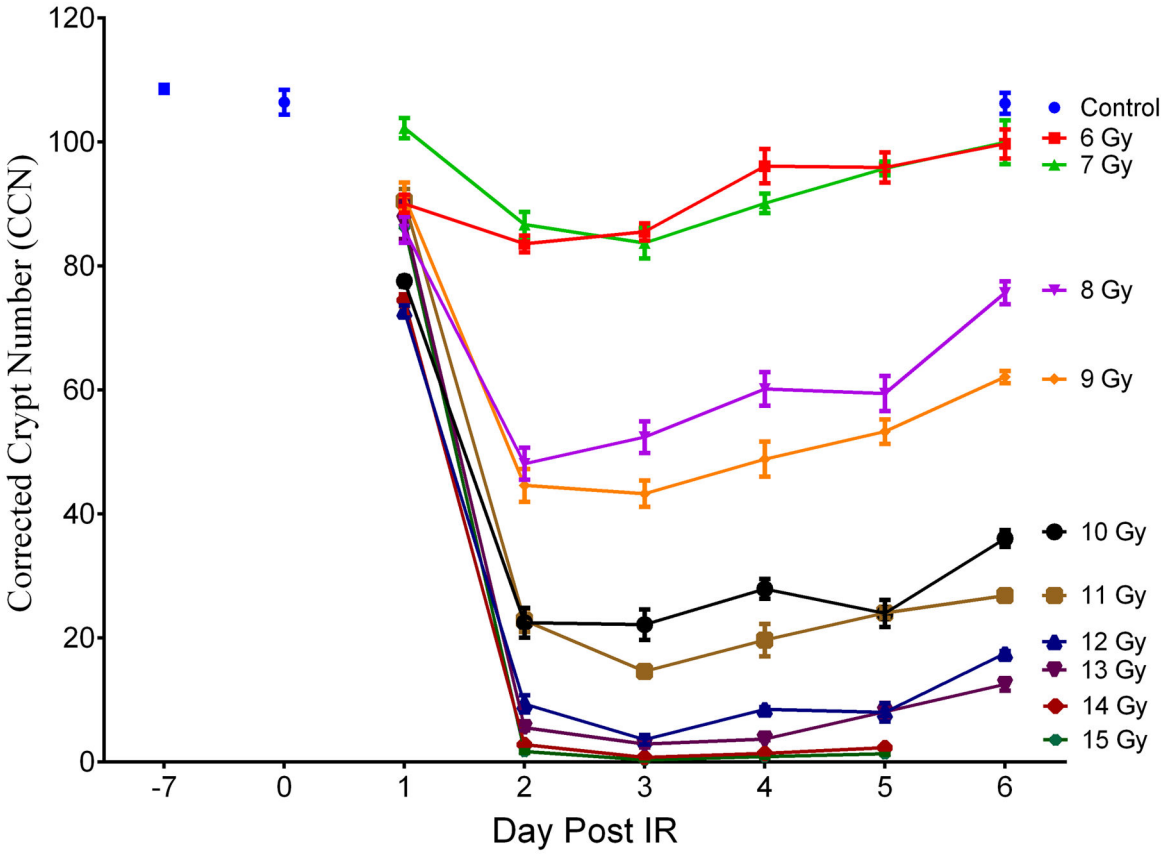

Fig. 6.

H&E stained sections of mouse jejunum tissue taken at the time of necropsy. 20x magnification. The day under each H&E image corresponded to the day post IR for the specific TBI dose which was designated to the left of the images. The images corresponded to non-irradiated control and representative cross sections of TBI doses 6, 8, 10, 12, and 14 Gy at days 2, 4, and 5/6 post-IR.

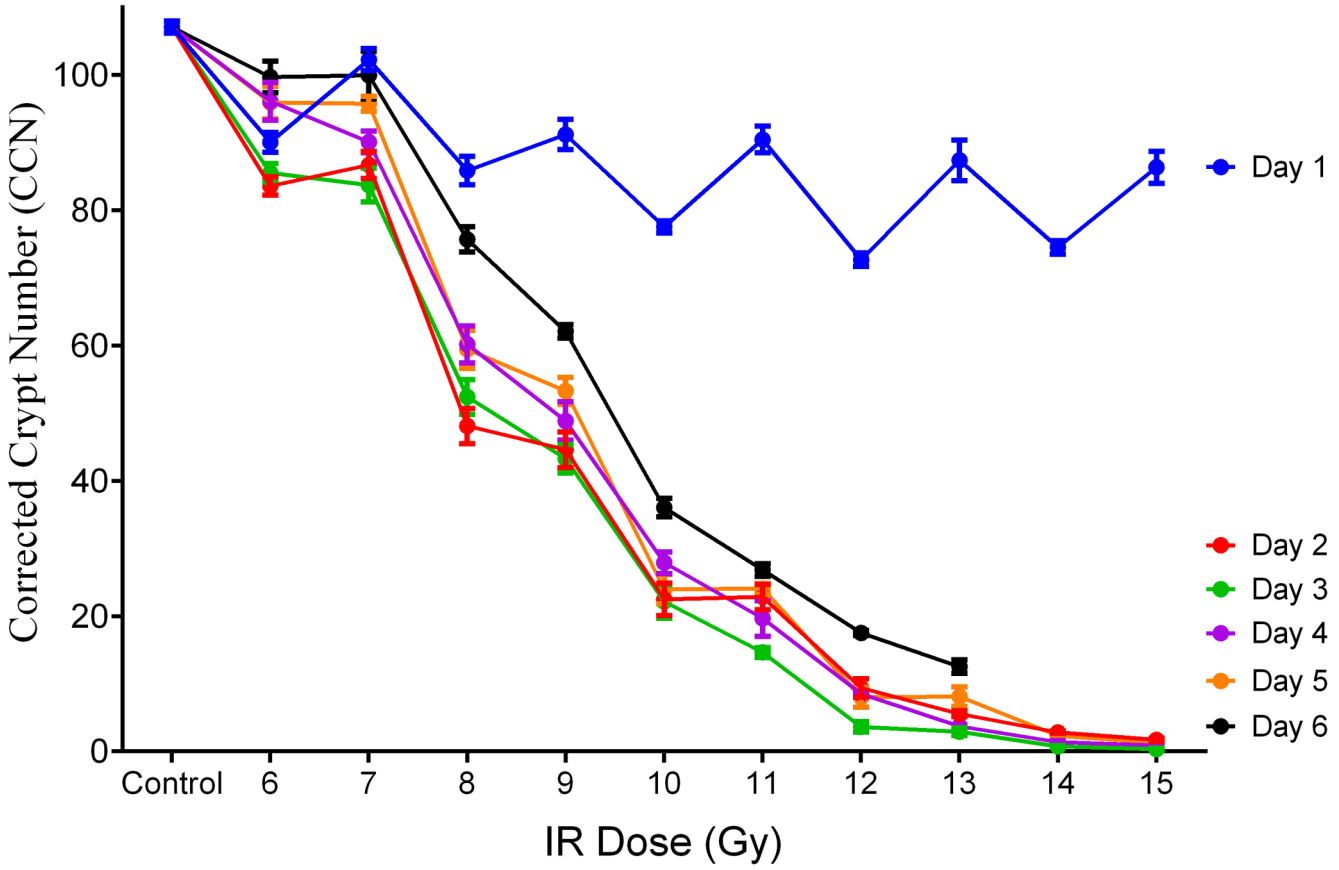

Fig. 7.

Corrected crypt number (CCN) expressed as a function of day per IR. Day −7 corresponded to age-matched non-irradiated control mice 7 days prior to IR. Day 0 corresponded to age-matched non-irradiated control mice just prior to the IR event. CCN values for day 6 at 14 and 15 Gy were not accessible due to euthanasia criteria and were sampled on day 5. Values were expressed in mean ± sem. Refer to Table S5 for tabulated values for concentrations, error, and number of independent samples.

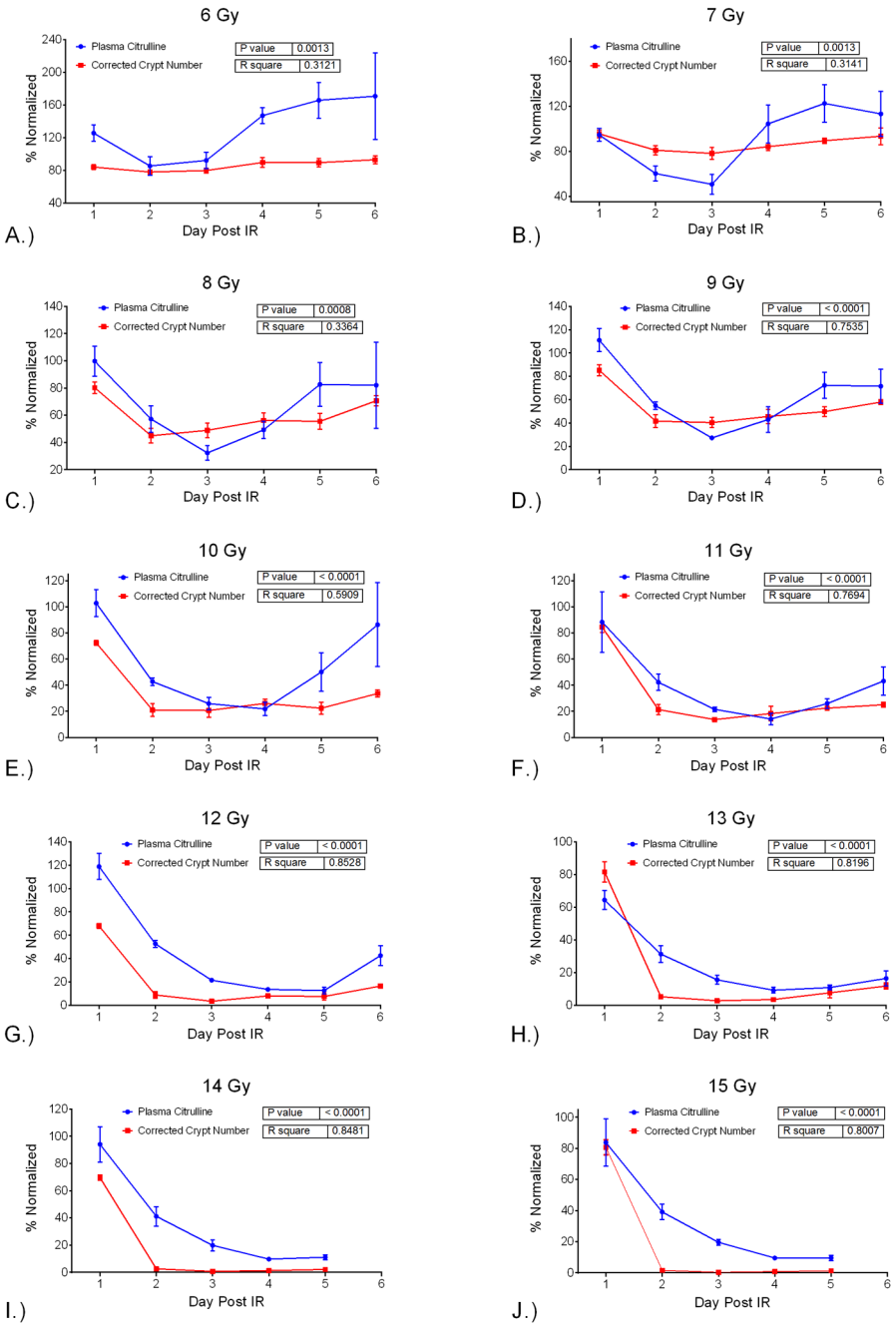

Fig. 8.

Corrected crypt number (CCN) values expressed as a function of IR dose per day. Control was the mean of CCN from all control time points (day −7, day 0 and day 6; n=15). CCN values for day 6 at 14 and 15 Gy were not accessible due to euthanasia criteria and were sampled on day 5. Values were expressed in mean ± sem.

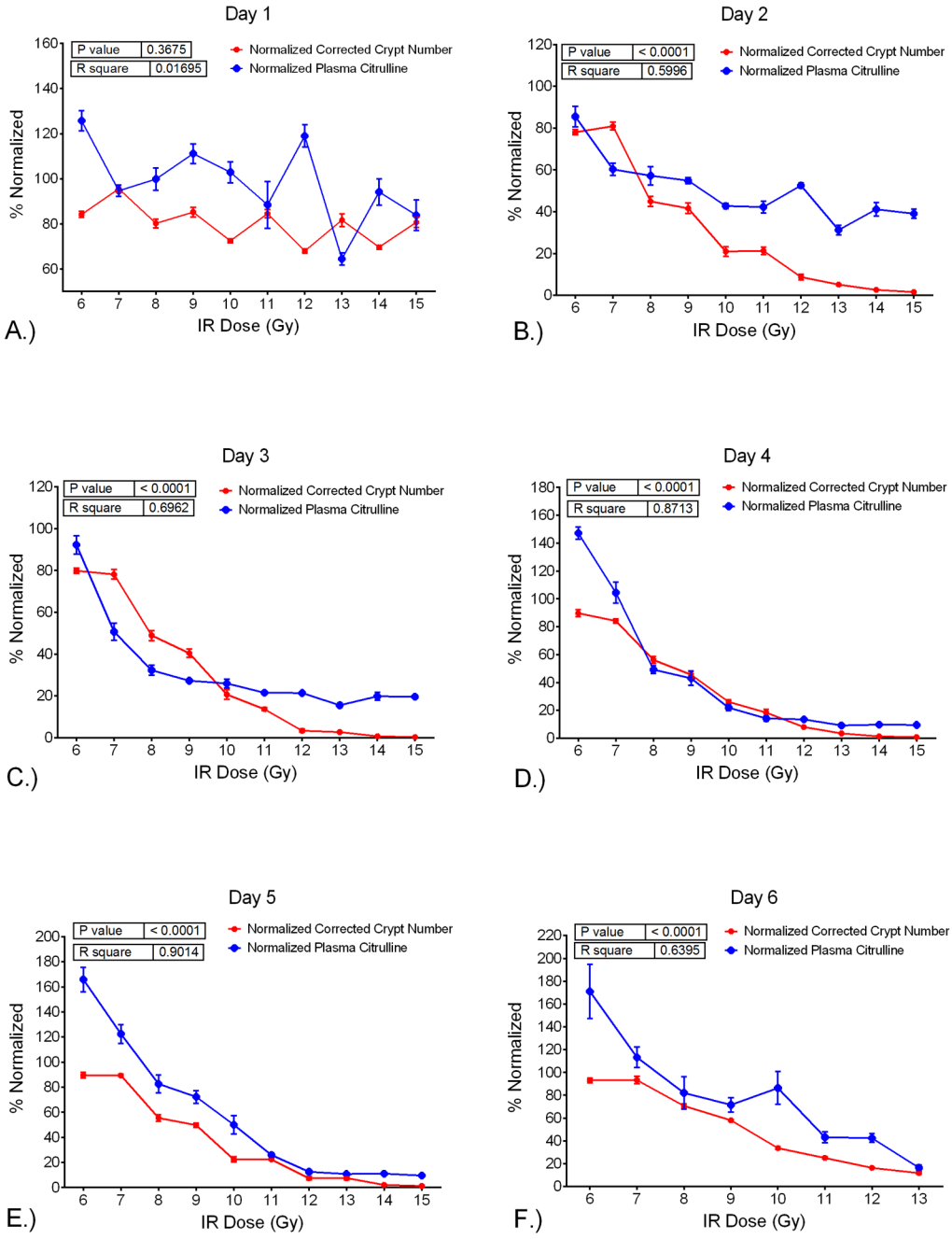

Fig. 9.

Normalized (%) values for plasma citrulline and CCN versus the day post IR. Plot shows plasma citrulline and CCN at IR dose versus the day post IR. Inset displays *p-value* and R^2 generated via linear regression analysis comparing plasma citrulline and CCN at a given dose over days 1–6, except 14 Gy and 15 Gy which are over days 1–5. A.) 6 Gy, B.) 7 Gy, C.) 8 Gy, D.) 9 Gy, E.) 10 Gy, F.) 11 Gy, G.) 12 Gy, H.) 13 Gy, I.) 14 Gy, J.) 15 Gy.

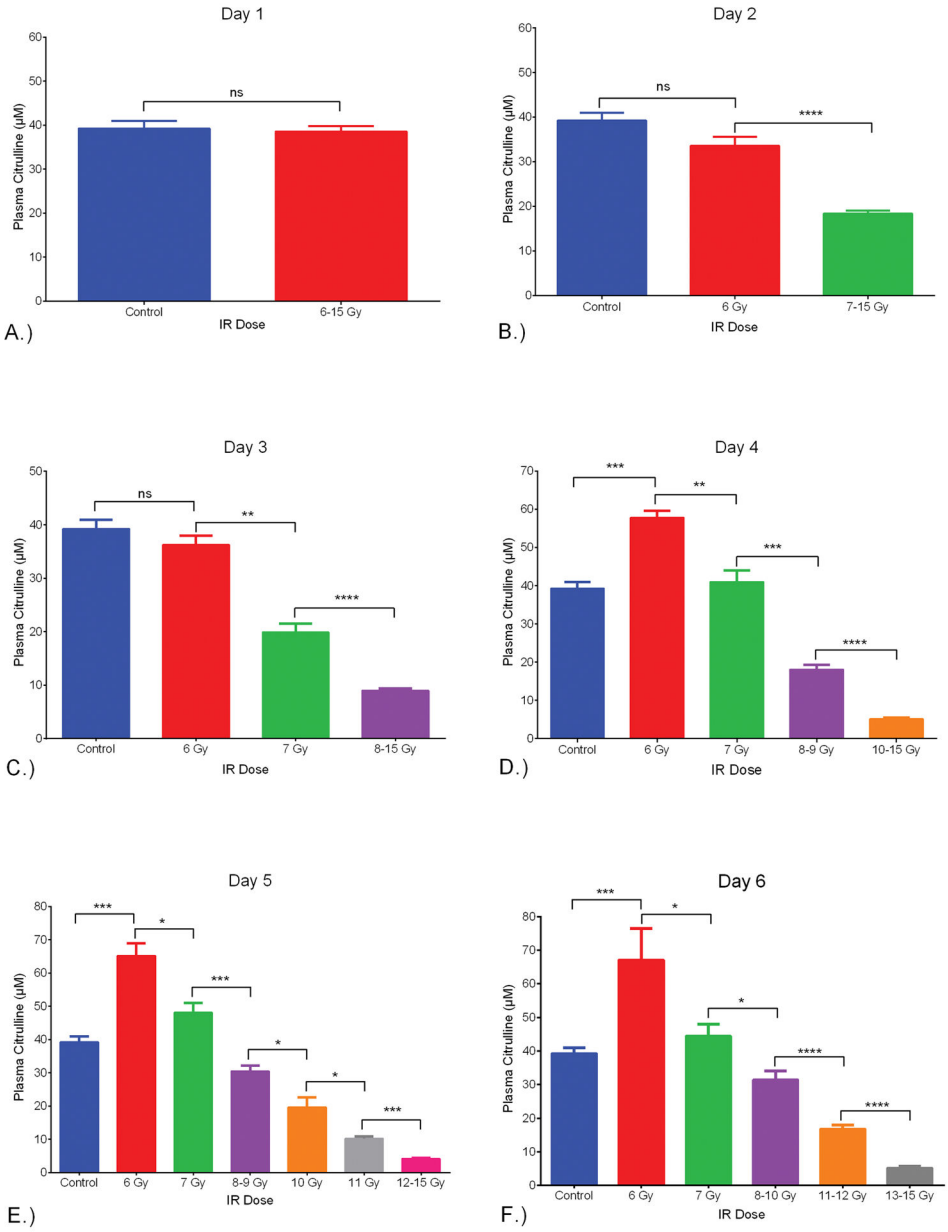

Fig. 10.

Normalized (%) values for plasma citrulline and CCN versus the IR-dose. Plot shows plasma citrulline and CCN for day versus the IR dose. Inset displays *p-value* and R^2 generated via linear regression analysis comparing plasma citrulline and CCN for a given day over 6–15 Gy, except day 6 which is over 6–13 Gy. A.) day 1, B.) day 2, C.) day 3, D.) day 4, E.) day 5, F.) day 6.

Table 1

Linear regression analysis for plasma citrulline versus IR dose per day. The day corresponded to the number of days post IR. The estimate referred to the estimated decrease in IR dose (Gy) per one unit (1 μM) increase in citrulline concentration. The *p-value* of <0.05 (two-sided test) was considered significant. The R^2 value was generated via linear regression analysis.

Plasma Citrulline Response to IR per Day

	Estimate (Gy)	*p-value*	R^2
Day 1	0.17	0.0005	0.223
Day 2	0.36	<0.0001	0.587
Day 3	0.25	<0.0001	0.573
Day 4	0.14	<0.0001	0.709
Day 5	0.13	<0.0001	0.821
Day 6	0.11	<0.0001	0.727

Table 2

Linear regression analysis for CCN versus IR dose per day. The day corresponded to the number of days post IR. The estimate referred to the estimated decrease in IR dose (Gy) per ten unit increase in CCN. The *p-value* of <0.05 (two-sided test) was considered significant. The R^2 value was generated via linear regression analysis.

Corrected Crypt Number Response to IR per Day

	Estimate (Gy)	*p-value*	R^2
Day 1	0.15	0.0003	0.245
Day 2	0.88	<0.0001	0.875
Day 3	0.84	<0.0001	0.880
Day 4	0.79	<0.0001	0.902
Day 5	0.82	<0.0001	0.891
Day 6	0.66	<0.0001	0.949

Table 3

Linear regression analysis for plasma citrulline versus CCN per IR dose over days 1 to 6. IR doses 14 and 15 Gy covered days 1 to 5. The estimate referred to the estimated increase in CCN value per one unit (1 μM) increase in plasma citrulline. The *p-value* of <0.05 (two-sided test) was considered significant. The R^2 value was generated via linear regression analysis.

Plasma Citrulline versus Corrected Crypt Number

IR Dose	Estimate (CCN)	*p-value*	R^2
6 Gy	0.25	0.0013	0.312
7 Gy	0.39	0.0013	0.314
8 Gy	0.76	0.0008	0.336
9 Gy	1.35	<0.0001	0.754
10 Gy	1.18	<0.0001	0.591
11 Gy	2.22	<0.0001	0.769
12 Gy	1.54	<0.0001	0.853
13 Gy	3.63	<0.0001	0.820
14 Gy	2.16	<0.0001	0.848
15 Gy	2.65	<0.0001	0.801

Table 4

Linear regression analysis for plasma citrulline versus CCN per day over IR doses of 6–15 Gy. Day 6 covered IR doses of 6–13 Gy. The day corresponded to the number of days post the IR event. The estimate referred to the estimated increase in CCN value per one unit (1 μM) increase in plasma citrulline. The *p-value* of <0.05 (two-sided test) was considered significant. The R^2 value was generated via linear regression analysis.

Plasma Citrulline versus Corrected Crypt Number

Day Post-IR	Estimate (CCN)	*p-value*	R^2
Day 1	0.15	0.3675	0.017
Day 2	3.85	<0.0001	0.600
Day 3	3.02	<0.0001	0.696
Day 4	1.81	<0.0001	0.871
Day 5	1.62	<0.0001	0.901
Day 6	1.61	<0.0001	0.640